A Miniaturized Interdigital Bandpass Filter for Intentional Electromagnetic Interference Applications

Abirami B, Prerna Saxena and Premkumar K.
Department of Electronics and Communication Engineering
Indian Institute of Information Technology, Design and Manufacturing, Kancheepuram
Chennai, India
Email: {cds19m001, prerna.saxena, kpk}@iiitdm.ac.in

***Abstract*—We propose a compact bandpass filter over 0.52-2.07 GHz at the receiver front-end of an intentional electromagnetic interference detection system. We design the filter using five microstrip stubs arranged in interdigital configuration along with a dumbbell shaped defected ground structure. We design the proposed filter on FR4 substrate with a relative permittivity of 4.4 and a thickness of 1.6 mm. We obtain a 3dB fractional bandwidth of 119.96%. The proposed filter exhibits a return loss $>$12 dB, an insertion loss $\approx$0.922 dB and a flat group delay over the entire bandwidth. Also, the proposed filter is compact and occupies an area of 3.55 $\times$ 1.557 cm^2. As compared to the state-of-the-art designs, the proposed bandpass filter is highly miniaturized, easy to fabricate and exhibits good performance.**

***Index Terms*—Intentional electromagnetic interference, interdigital bandpass filter, defected ground structure.**

I. Introduction

Electrical and electronic systems constitute an indispensable part of the critical infrastructure such as transport systems, power grids, communication systems, healthcare, water supply etc. These systems are vulnerable to an emerging threat from high power electromagnetic pulses which is known as Intentional Electromagnetic Interference (IEMI). IEMI is defined as "The intentional malicious generation of electromagnetic energy introducing noise or signals into electric and electronic systems, thus disrupting, confusing or damaging these systems for terrorist or criminal purposes"[1-2]. Most of the research in IEMI has primarily focused on susceptibility analysis of electronic systems to an IEMI attack. The investigations on threat detection and mitigation have been very limited.

IEMI attacks cause upset, temporary performance degradation or permanent damage to electrical or electronic systems. The frequency range from 0.5-2 GHz is most likely to be used to stage an IEMI attack because most of the circuits and coupling paths (front-door as well as back-door) are resonant in this range. Thus, for the receiver front-end of an IEMI detection and diagnostic system, a bandpass filter would be required to restrict the received signal bandwidth over 0.5-2 GHz. This necessitates the design of a compact planar bandpass filter over 0.5-2 GHz. The bandpass filter is required to have low insertion loss along with small size and microstrip filters are preferred for this purpose [3].

Several investigations on the design of bandpass filters have been carried out in the literature. In [4], a microstrip bandpass filter is proposed with zero degree feed structure and shorted stub-loaded tri-section stepped impedance resonator. This gives a wider stopband and sharp roll-off but the in-band performance suffers from lower bandwidth and higher insertion loss. In [5], multilayer liquid crystal polymer technology is used to reduce the filter size over 0.5-2 GHz. However, the fabrication process is very complex and expensive. Recently, research on coupled resonator filters is being carried out to improve the bandwidth and to reduce filter size in the low frequency ranges. Stepped coupled lines and short circuited stubs are used to design a bandpass filter over 0.65-1.42 GHz in [6]. Open and short circuited stubs are employed in [7] to design a bandpass filter over 0.5-1.9 GHz. However, the filters proposed in [6] and [7] occupy very large area. Slot line resonators with a T-shaped feed in [8] and fork-form resonators in [13] are used to achieve a compact size. However, they are designed for a comparatively higher frequency range. Since the operating frequency range for IEMI is very low, the main design challenge lies in reducing the filter size while maintaining a good performance and ease of fabrication.

In this paper, we propose a miniaturized Interdigital Bandpass Filter (IDBPF) with dumbbell shaped Defective Ground Structure (DGS) over 0.52 - 2.07 GHz. The fractional bandwidth of the proposed filter is 119.69%. The rest of the paper is organized as follows. In section II, the proposed filter geometry and design details are elaborated. The detailed parametric studies and their effects on the filter frequency response are analysed and discussed in Section III. Also, the lumped equivalent circuit for the proposed filter is presented in Section III along with a comparison between the frequency response obtained from circuit simulation and full-wave simulation. In addition, the performance summary of the proposed filter and a comparison with the state-of-the-art designs is also presented in Section III. This work is concluded in Section IV.

978-1-6654-4177- 3/21/$31.00 ©2021 IEEE

978-1-6654-4177-3/21/$31.00 ©2021 IEEE

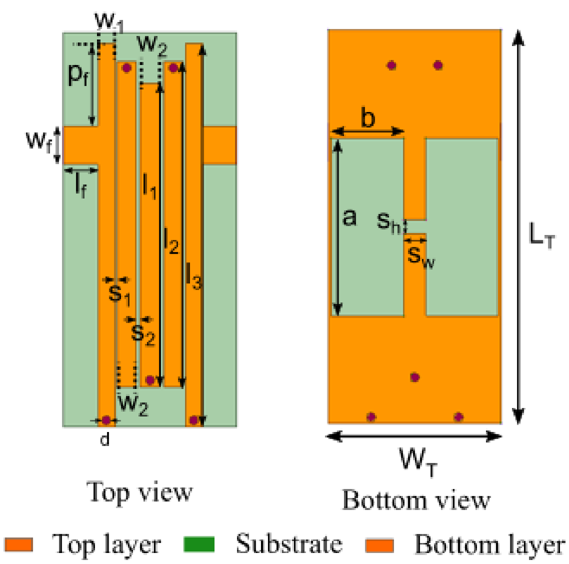

Fig. 1: Geometry of the proposed bandpass filter.

II. Proposed Interdigital Bandpass Filter Design

The proposed interdigital bandpass filter (IDBPF) with defected ground structure (DGS) is shown in Fig. 1. The proposed design is obtained in two steps. In the first step, a wideband fifth order bandpass filter is designed using five microstrip stubs arranged in interdigital configuration. Further, a dumbbell shaped defected ground structure is introduced in the bandpass filter. The effect of DGS on size reduction and bandwidth enhancement is studied by comparing it to the filter response without DGS, as shown in Fig. 2.

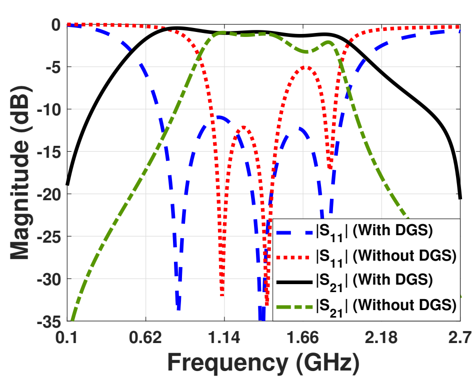

Fig. 2: Performance comparison of BPF with and without DGS.

The proposed filter is designed on FR4 substrate with thickness, relative permittivity (ϵ_r) and loss tangent of 1.6 mm, 4.4 and 0.02 respectively. The thickness of the copper is 0.035 mm. The area of the filter is 3.55 $\times$ 1.557 cm^2 ($L_T \times W_T$). The optimized dimensions of the proposed bandpass filter are described below.

The 50Ω microstrip feed line length (l_f) = 3.08 mm and width (w_f) = 3.43 mm. The feed lines are attached to the resonators at p_f = 7.42 mm away form the start of the resonator. The first and fifth resonators are of length (l_3) = 33.5 mm and width (w_1) = 1.53 mm. The second and fourth resonators are of length (l_2) = 28.31 mm and width (w_2) = 1.75 mm and the center resonator is of length (l_1) = 26.31 mm and width (w_2) = 1.75 mm. The spacing between the resonators is s_1 = 0.2 mm and s_2 = 0.35 mm. Vias are introduced in the alternate sides of the resonators and their diameter is d = 0.8 mm. The optimized dimensions of the dumbbell shaped defected ground structure are as follows: a = 16 mm, b = 6.55 mm, s_h = 1.3 mm and s_w = 2 mm.

III. Results and Discussion

The proposed filter is designed and simulated in ANSYS HFSS. A detailed parametric analysis is carried out to optimize the dimensions of the proposed IDBPF with DGS. The parameters that have significant effect on its frequency response are as follows: length of the resonators (l_1,l_2,l_3), spacing between the resonators (s_1,s_2), feed position (p_f), DGS slot length (a) and width (b), and the gap height (s_h) & width (s_w). In the following analysis, only the parameter under consideration is varied, all other parameters are set to their optimum value.

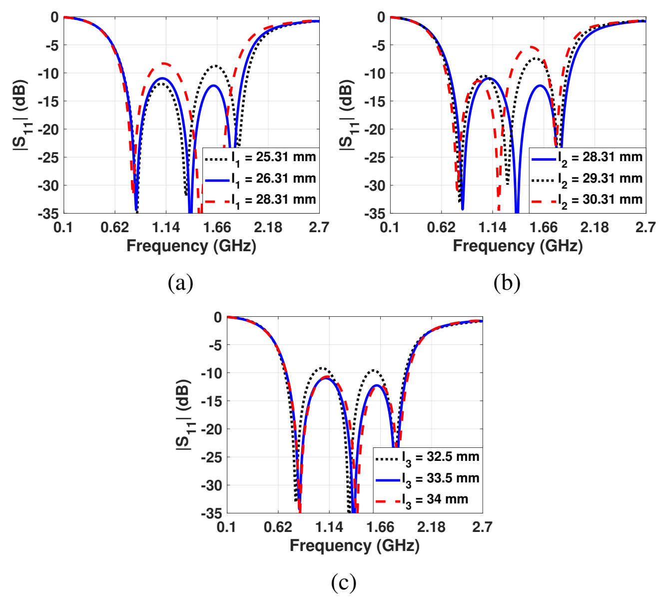

Fig. 3: Effect of variation in resonator length on ($|S_{11}|$) of the proposed IDBPF with DGS: (a) l_1, (b) l_2 and (c) l_3.

1) Effect of variation in the length of the resonators: The effect of varying the length of the resonators on the reflection coefficient ($|S11|$) of the proposed filter is depicted in Fig. 3. It is observed that as l_3 increases, the capacitance tends to increase. As a result, the upper cut-off frequency increases marginally, and the stopband roll-off increases. As l_2 increases, the circuit becomes more inductive due to which the upper cut-off frequency reduces. Also impedance mismatch occurs and the passband shifts to the left. As the length of the middle resonator (l_1) increases, there is a reduction in the bandwidth of the passband. In addition, impedance mismatch also increases.

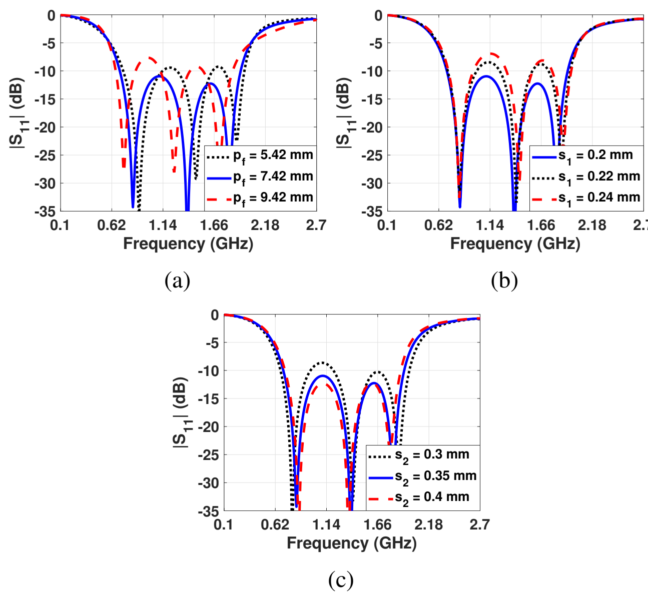

Fig. 4: Effect on $|\mathrm{S}_{11}|$ of the proposed IDBPF with DGS due to: (a) $\mathrm{p_f}$, (b) s_1 and (c) s_2.

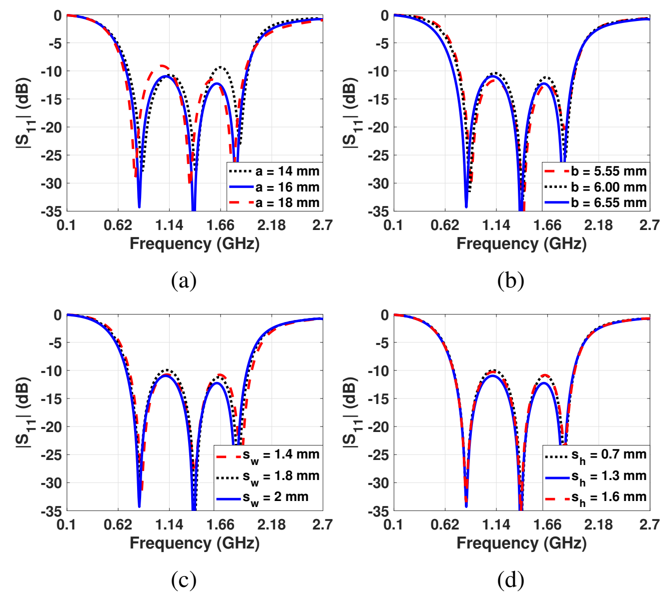

Fig. 5: Effect on $|\mathrm{S}_{11}|$ of the proposed IDBPF with DGS due to: (a) slot length (a), (b) slot width (b), (c) gap width $(\mathrm{s_w})$, and (d) gap height $(\mathrm{s_h})$.

2) Effect of the feed position: The effect of the feed position $(\mathrm{p_f})$ on the reflection coefficient $(|\mathrm{S}_{11}|)$ of the proposed filter is shown in Fig. 4(a). The greater the distance of the feed from the start of the resonator, the greater is the inductance and this reduces the lower cut-off frequency of the filter.

3) Effect of the spacing between the resonators: The effective capacitance of the circuit is influenced by the spacing between the resonators, resulting in a range of filter responses as shown in Figs. 4(b) and 4(c). It is seen that impedance mismatch occurs as the s_1 between l_3 and l_2 increases. Also, as the s_2 between the l_1 and l_2 increases, the effective capacitance tends to reduce, causing the passband bandwidth and impedance mismatch to increase.

4) Effect of the DGS parameters: As seen in Fig. 5(a), as the DGS slot length (a) increases, the passband bandwidth increases. An increase in the DGS width (b) leads to smaller capacitance, thus the lower cut-off frequency shifts towards 0.5 GHz as shown in Fig. 5(b). While the capacitance is affected by the DGS slot dimensions, the inductance is affected by the gap dimensions. Figures 5(c) and 5(d) show that the $\mathrm{s_w}$ affects the lower cut-off frequency, while $\mathrm{s_h}$ moves the poles towards the higher frequency, resulting in a minor shift in the passband.

The optimized dimensions of the proposed IDBPF with DGS are obtained from these parametric studies. The reflection coefficient ($|S_{11}|$) and transmission coefficient ($|S_{21}|$) magnitudes as a function of frequency for the proposed filter are plotted in Fig. 6. The proposed filter exhibits a passband from 0.52 - 2.07 GHz. The reflection coefficient ($|S_{11}|$) < -12 dB is obtained over the passband which shows a good impedance matching.

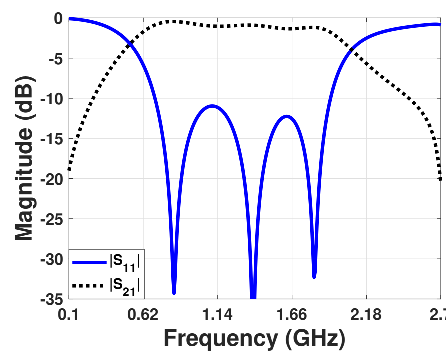

Fig. 6: Reflection and transmission coefficient versus frequency for the proposed IDBPF with DGS.

The lumped equivalent circuit for the proposed bandpass filter is depicted in Fig. 7(a). It is designed and simulated in AWR Design Environment. The optimized component values are as follows: $\mathrm{C1} = 0.96\mathrm{pF}$, $\mathrm{C2} = 3.25\mathrm{pF}$, $\mathrm{C3} = 3.25\mathrm{pF}$, $\mathrm{L1} = 32\mathrm{nH}$, $\mathrm{L2} = 28.6\mathrm{nH}$, $\mathrm{L3} = 80\mathrm{nH}$, $\mathrm{L4} = 4.5\mathrm{nH}$ and $\mathrm{L5} = 6.9\mathrm{nH}$. The reflection coefficient ($|S_{11}|$) and transmission coefficient ($|S_{21}|$) magnitudes versus frequency are plotted in Fig. 7(b). It is seen from Fig. 8 that the frequency response of the proposed bandpass filter obtained from circuit simulation and full-wave simulation are in good agreement. The group delay versus frequency for the proposed filter is shown in Fig. 9. It is seen that the group delay is $<$1.3 ns and is almost flat over 0.5-2 GHz. This shows that the proposed filter has a linear phase response.

The prototype of the proposed filter is fabricated. The photographs of the fabricated filter and the measurement set-up are shown in the Fig. 10(a)-(c). For the appropriate frequency

TABLE I: Comparison of the proposed bandpass filter with the state-of-the-art designs.

Technique	3dB Frequency Range (GHz)	Fractional Bandwidth (%)	Substrate ϵ_r, Thickness (mm)	Return loss (dB)	Insertion loss (dB)	Area (λ_{g0}^2)
Stepped coupled lines with short-circuited stubs [6]	0.65 - 1.42	74.4	4.4, 1.6	>18	<1.9	0.214
Open and short circuited stubs [7]	≈(0.5 - 1.9)	≈116.67	2.65, 0.508	>10	<0.3	0.092
Slot line resonators using T-shaped microstrip feed [8]	1.65 - 2.94	56.3	2.2, 0.381	>13.2	1.2	0.054
Dual mode resonators and interdigital capacitors [9]	0.32 - 0.42	26.7	10.2, 1.28	16.5	0.51	0.049
Meander coupled lines [10]	0.29 - 0.47	48.5	10.2, 1.28	17.5	0.43	0.045
Interdigital capacitor [11]	0.65 - 1.2	63	4.4, 0.8	17	0.59	0.055
ladder topology circuit [12]	0.81 - 2.69	108	9.67, 0.5	14	0.29	0.343
Interdigital BPF with DGS [This work]	0.52 - 2.07	119.69	4.4, 1.6	>12	≈0.922	0.042

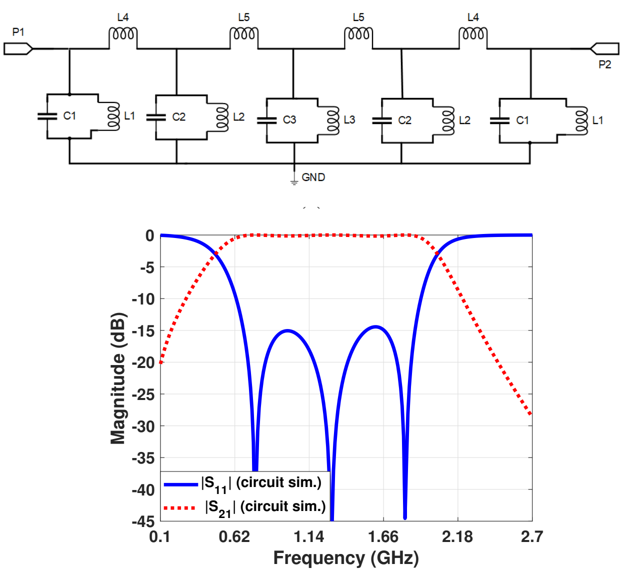

(b)

Fig. 7: (a) Lumped equivalent circuit for the proposed IDBPF with DGS, (b) reflection and transmission coefficients.

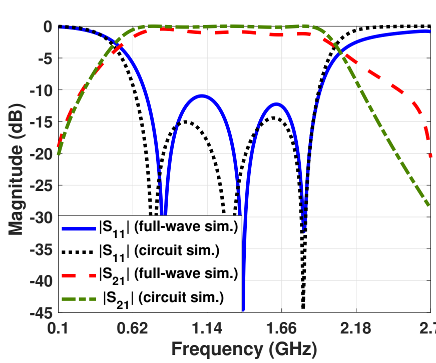

Fig. 8: Performance comparison between circuit simulation and full-wave simulation.

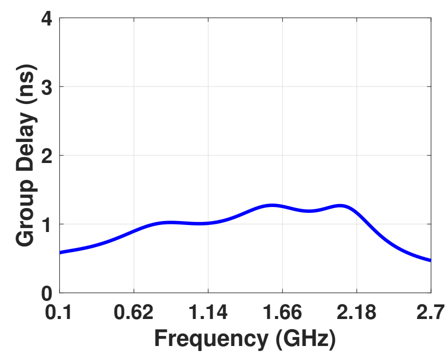

Fig. 9: Group delay for the proposed IDBPF with DGS.

range, the scattering parameters of the fabricated prototype of the proposed miniaturized IDBPF with Dumbbell shaped DGS are measured using a Vector Network Analyser (VNA).

Fig. 11 depicts the simulated and measured scattering parameters of the proposed IDBPF with DGS. It is seen that the measured results are in very good agreement with the simulations. The slight deviation between the simulation and measurement is attributed to the fabrication tolerance and connector losses.

The performance summary along with the comparison of the proposed filter with the state-of-the-art designs is summarized in Table I. The filter proposed in [6] operates over 0.65-1.42 GHz and has a return loss > 18dB. However, as compared to the filter proposed in this work, it is narrowband with a fractional bandwidth of 74.4% and has a higher insertion loss. The filter proposed in [7] employs open and short circuited stubs and operates over the similar frequency range as the filter proposed in this work. However, the area of the proposed filter in [7] is 3.94 times greater as compared to this work. The 3 dB bandwidth in [8] is lesser than the proposed work. In addition, the filter designed in [8] shows a higher insertion loss of 1.2 dB. Though [9-11] have

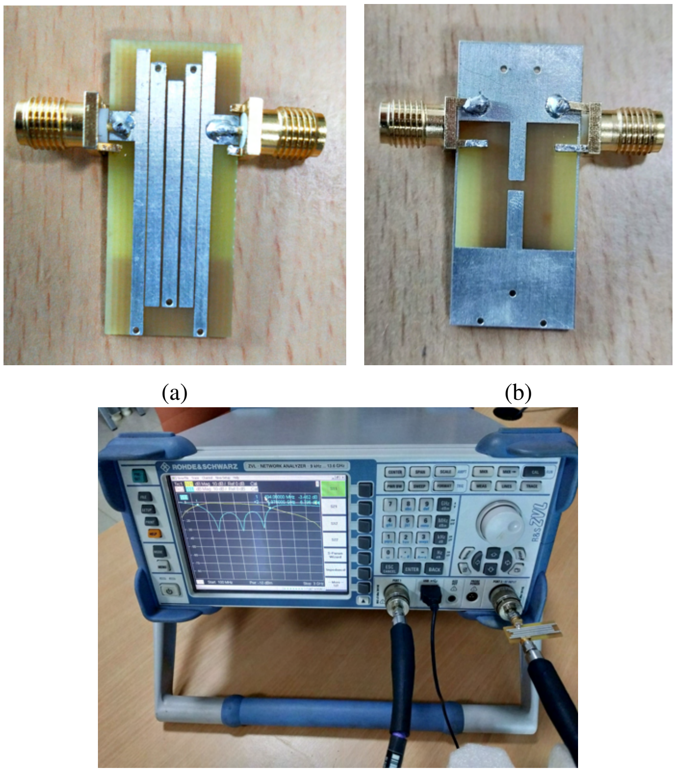

(a) (b)

(c)

Fig. 10: Fabricated prototype: (a) Top view, (b) Bottom view and (c) Measurement set-up.

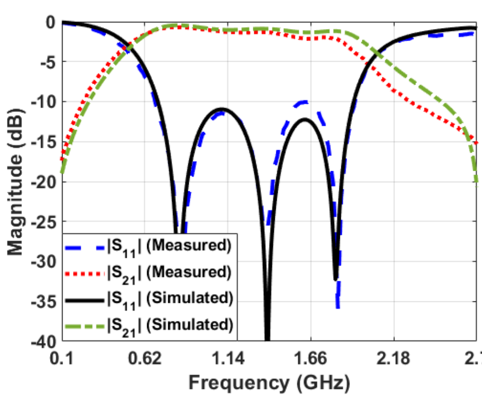

Fig. 11: Simulated and measured scattering parameters of the proposed filter.

better insertion and return losses, the fractional bandwidth is much smaller than the proposed filter. In terms of bandwidth and size, the filter designed is better than [12]. Hence, the proposed bandpass filter shows good performance in terms of return loss, insertion loss and 3dB bandwidth. Also, it is compact and occupies much lesser area as compared to the state-of-the-art approaches.

IV. Conclusion

In this paper, we proposed a miniaturized interdigital bandpass filter with defected ground structure over 0.52-2.07 GHz. The filter was designed using five microstrip stubs arranged in interdigital configuration and a dumbbell shaped defected ground structure. The proposed filter gives a return loss >12 dB and an insertion loss of approximately 0.922 dB over the passband. In addition, it is compact and occupies an area of 5.52 cm^2. The proposed bandpass filter exhibits better performance in terms of return loss, insertion loss and 3dB bandwidth, and occupies much lesser area as compared to the state-of-the-art filter designs.

Acknowledgment

This work was supported by the SERB Core Research Grant CRG/2019/004832.

References

[1] C.E. Baum, "Maximization of Electromagnetic Response at a Distance", *IEEE Transactions on Electromagnetic Compatibility*, vol.34, no.3, Aug. 1992.

[2] W.A. Radasky, C.E. Baum and M.W.Wik, "Introduction to the Special Issue on High-Power Electromagnetics (HPEM) and Intentional Electromagnetic Interference (IEMI)", *IEEE Transactions on Electromagnetic Compatibility*, vol.46, no.3, Aug. 2004.

[3] D.M. Pozar, "Microwave Filters," in *Microwave Engineering*, 4th ed. USA: Wiley,2011, ch.8, pp. 381-437.

[4] D. Li, J.A. Wanga, Z. Chen, Y. Zhang , M.C. Tang, L. Yang, "Compact microstrip bandpass filter with sharp roll-off and broad stopband using modified 0deg feed structure", *International Journal of Electronics and Communications (AEU)*, vol.109, pp. 17-22, Sep. 2019.

[5] S. Qian,and J. Hong, "Miniature Quasi-Lumped-Element Wideband Bandpass Filter at 0.5–2-GHz Band Using Multilayer Liquid Crystal Polymer Technology", *IEEE Transactions on Microwave Theory and Techniques*, vol.60, no.9, Sep. 2012.

[6] C.W. Tang, C.T. Tseng, S.H. Chiu, and P.H. Wu, "Design of Wide Passband/Stopband Microstrip Bandpass Filters With the Stepped Coupled Line", *IEEE Transactions on Microwave Theory and Techniques*, vol.61, no.3, Mar. 2013.

[7] X. Gao, W. Feng, and W. Che, Senior Member, "Compact Ultra-Wideband Bandpass Filter With Improved Upper Stopband Using Open/Shorted Stubs", *IEEE Microwave and Wireless Components Letters*, vol.26, no.2, Feb. 2017.

[8] P. Mondal, and A. Chakrabarty, "Compact Wideband Bandpass Filters With Wide Upper Stopband", *IEEE Microwave and Wireless Components Letters*, vol.17, no.1, Jan. 2007.

[9] V. K. Killamsetty and B. Mukherjee, "Miniaturised highly selective wide-band bandpass filter using dual-mode resonators and inter digital capacitors", *IET Electronics Letters*,vol. 53, no. 17, pp. 1209-1211, 2017.

[10] V. K. Killamsetty and B. Mukherjee, "Miniaturized highly selective bandpass filter with a very wide stopband using meander coupled lines", *IET Electronics Letters*, vol. 53, no. 13, pp. 889-890, 2017.

[11] S. Sen and T. Moyra, "Interdigital Capacitor Based Compact Microstrip Bandpass Filter with Wide Stopband", *IETE Journal of Research*, vol. 67, no. 1, pp. 82-89, 2018.

[12] J. Dai et al., "HTS Wideband Bandpass Filter Based on Ladder Topology Circuit and Microstrip Transformation," *IEEE Transactions on Applied Superconductivity*, vol. 31, no. 4, pp. 1-7, June 2021.

[13] H. Chen and Y.X. Zhang, "A Novel and Compact UWB Bandpass Filter using Microstrip Fork-Form Resonators", *PIER*, vol. 77, pp. 273-280, Aug. 2007.